

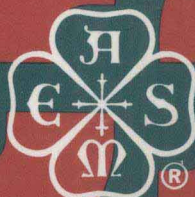
DE-Vol. 44-2

ADVANCES IN DESIGN AUTOMATION — 1992 —

VOLUME 2

Geometric Modeling, Mechanisms,
and Mechanical Systems Analysis

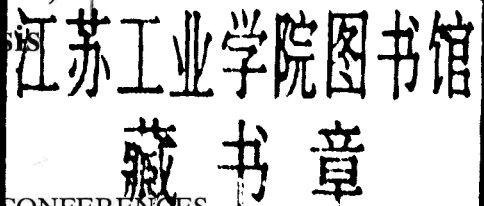
Edited By
D. A. HOELTZEL



ADVANCES IN DESIGN AUTOMATION — 1992 —

VOLUME 2

**Geometric Modeling, Mechanisms,
and Mechanical Systems Analysis**



presented at

THE 1992 ASME DESIGN TECHNICAL CONFERENCES

18TH DESIGN AUTOMATION CONFERENCE

SCOTTSDALE, ARIZONA

SEPTEMBER 13-16, 1992

sponsored by

THE DESIGN ENGINEERING DIVISION, ASME

edited by

DAVID A. HOELTZEL

COLUMBIA UNIVERSITY

THE AMERICAN SOCIETY OF MECHANICAL ENGINEERS

United Engineering Center 345 East 47th Street New York, N.Y. 10017

Statement from By-Laws: The Society shall not be responsible for statements or opinions advanced in papers . . . or printed in its publications (7.1.3)

ISBN No. 0-7918-0938-2

Library of Congress
Catalog Number 89-45945

Copyright © 1992 by
THE AMERICAN SOCIETY OF MECHANICAL ENGINEERS
All Rights Reserved
Printed in U.S.A.

FOREWORD

The papers which appear in this volume were presented at the 18th Annual ASME Design Automation Conference held in Phoenix/Scottsdale, Arizona, September 13–16, 1992. This conference was sponsored by the Design Engineering Division of the American Society of Mechanical Engineers, and was organized by the Design Automation Committee.

The underlying goal of the ASME Design Automation Conference is to provide a lively forum for the interchange of technical ideas and presentation of timely and high quality technical papers in the area of Mechanical Design Automation. As the field of mechanical design continues to unfold and evolve into more modern themes that encompass Geometric Modeling of Features and Tolerances, Manufacturing Processes, Concurrent Engineering, Automated Structural Shape Generation, and New Optimization Algorithm, I am happy to report that each of these topics has been appropriately represented in a technical session.

The conference has a total of 18 technical sessions comprising a total of 93 papers. This second volume contains 49 papers on topics that include the Geometric Modeling of Curves, Surfaces, Tolerances and Features, Mechanical Systems Analysis, Compliant Mechanisms and Mechanical Advantage, Robotics, and Mechanical Design Applications.

As the papers review chairman, I would like to express my sincere thanks to Joe Davidson, who has courageously undertaken and skillfully orchestrated the entire Design Technical Conference, to Brian Gilmore, who served as foreign papers chairman, and to Bahram Ravani, Gary Gabriele and Panos Papalambros, of the ASME Design Automation Committee, each of whom provided expert guidance for me from their past experiences in chairing this conference. Their help proved invaluable to me. I would also like to thank Barbara Signorelli and the ASME Technical Publications Department for coordinating and organizing the papers for publication in the bound volumes.

Finally, I would like to thank all those who contributed the fruits of their research labor for presentation at the conference, as well as those who took time from their busy lives to review papers for the conference. The timely, thoughtful and conscientious completion of the reviews continues to ensure the overall quality of the conference.

David A. Hoeltzel
Papers Review Chairman
Columbia University
New York, N.Y.

CONTENTS

MECHANISMS: MECHANICAL ADVANTAGE, COMPLIANCE AND LINK DESIGN

Second Order Design Sensitivity Analysis of Kinematically-Driven Mechanical Systems <i>Qiushi Cao and Prakash Krishnaswami</i>	1
Determination of Significance of Stress Stiffening Effects in Flexible Multibody Dynamic Systems <i>Jeha Ryu, Sang Sup Kim, and Sung-Soo Kim</i>	7
An Alternative Approach to Mechanical Advantage for the Analysis of a Multiple-Input Multiple-Output Mechanical Device <i>M. M. Ogot and B. J. Gilmore</i>	15
Automated Optimal Shape Design System of Planar Link Mechanisms Using an Object-Oriented Modeling Method <i>Kikuo Fujita, Shinsuke Akagi, and Kazunori Tsujimoto</i>	21
A Methodology for Compliant Mechanisms Design: Part I — Introduction and Large-Deflection Analysis <i>A. Midha, I. Her, and B. A. Salamon</i>	29
A Methodology for Compliant Mechanisms Design: Part II — Shooting Method and Application <i>I. Her, A. Midha, and B. A. Salamon</i>	39
An Introduction to Mechanical Advantage in Compliant Mechanisms <i>B. A. Salamon and A. Midha</i>	47

SYNTHESIS AND ANALYSIS OF LINKAGES AND GEAR TRAINS

Using Exact Gradients in Mechanism Design <i>J. Mariappan and S. Krishnamurty</i>	53
A Model for Mechanism Data Storage <i>Wan Wang</i>	61
Application of Expert System for a Compound Gear Train Design <i>Saiwei Yang and Kenny Yu</i>	67
Kinematic Synthesis of Ordinary and Epicyclic Gear Trains for a Prescribed Velocity Ratio <i>Ettore Pennestri</i>	75
A Simplified Approach for Force and Power-Flow Analysis of Compound Epicyclic Spur-Gear Trains <i>L. Saggere and D. G. Olson</i>	83

TOLERANCES, FEATURES AND VARIATIONAL GEOMETRY

ManuFEATURE: A Framework for Recognizing CAD Interactions in Design-for-Manufacturing Analysis <i>Rajit Gadh and Fritz B. Prinz</i>	91
B-Rep Feature Extraction Via Primitive Tracking <i>M. A. Ganter</i>	105
Computation of Spatial Displacements From Redundant Geometric Features <i>Q. J. Ge and B. Ravani</i>	113

Representing Geometric Variations in Complex Structural Assemblies on CAD Systems <i>Dari Shalon, David Gossard, Karl Ulrich, and David Fitzpatrick</i>	121
Attributed Graph Model for Geometric Tolerancing <i>Jami J. Shah and Bing-Chun Zhang</i>	133
TOLERANCE ANALYSIS AND ALLOCATION	
A Solid Boundary Based Tolerance Representation Model <i>S. Liu and Z. Dong</i>	141
Incorporating Geometrical Tolerances and Processing Inaccuracy Into Dimensioning and Tolerancing <i>Michel Prochet and Genbao Zhang</i>	151
CATI: A Computer Aided Tolerancing Interface <i>Rikard Söderberg</i>	157
Optimal Tolerance Allocation Over Multiple Manufacturing Alternatives <i>Jonathan Cagan and Thomas R. Kurfess</i>	165
GEOMETRIC MODELING, COMPUTER GRAPHICS AND VISION	
Computer Aided Modeling of Families and Family Members of Designed Parts <i>H. L. Johannesson</i>	173
Using Error Diffusion With Ordered Dither Matrix Method in Displaying Shaded Graphics <i>I. Her</i>	181
A Symmetrical Coordinate Frame on the Hexagonal Grid for Computer Graphics and Vision <i>I. Her</i>	187
A 3-D Vision System Model for Automatic Object Surface Sensing <i>Vassilios E. Theodoracatos and Dale E. Calkins</i>	191
CURVES AND SURFACES: INTERSECTIONS, BLENDING, JOINING AND DESIGN	
Parametric Surface Intersections for Geometric Modeling <i>J.-M. Chen, Yu Wang, E. L. Gursoz, and Fritz B. Prinz</i>	207
Intersection of Offset Surfaces of Parametric Patches <i>Yu Wang</i>	215
Intersection of Rays With Parametric Envelope Surfaces Representing Five-Axis NC Milling Tool Swept Volumes <i>Ashish P. Narvekar, Yunching Huang, and James H. Oliver</i>	223
Blending and Joining Using Cyclides <i>Y. L. Srinivas and Debasish Dutta</i>	231
A Geometric Framework for Optimal Surface Design <i>Frank C. Park</i>	237
SURFACES, SILHOUETTES AND TOPOLOGY IN GEOMETRIC MODELING	
Geometric Design and Fabrication of Developable Bezier Surfaces <i>R. M. C. Bodduluri and B. Ravani</i>	243
Boundary Surface Recovery From Skeleton Elements: Part I – Skeleton Curves <i>Sean M. Gelston and Debasish Dutta</i>	251
Boundary Surface Recovery From Skeleton Elements: Part II – Skeleton Surfaces <i>Sean M. Gelston and Debasish Dutta</i>	259
Geometrical and Topological Issues in NMT-Based Modeling <i>Mukul Saxena, Rajan Srivatsan, and Jonathan E. Davis</i>	267
Object Extent Determination for Algebraic Solid Models <i>M. A. Ganter and D. W. Storti</i>	275
MODELING AND PLANNING IN ROBOTICS	
Three Dimensional Robot Path Planning With Workspace Considerations <i>C. Y. Liu and R. W. Mayne</i>	285

A Computational Environment for Dextrous Workspace Analysis <i>J. Y. Wang and J. K. Wu</i>	293
Numeric-Symbolic Approach for Dynamic Modelling of Robotic Manipulators <i>Shou-wen Fan, Liju Xu, and Yong Chen</i>	303
Kinematic Evaluation of Robots for Assembly Tasks <i>Eyal Zussman, Moshe Shoham, and Ehud Lenz</i>	307
BUCKLING, FATIGUE AND STOCHASTIC DESIGN APPLICATIONS	
Design of an Aircraft Tire: A Study in Modeling Uncertainty <i>S. Vadde, S. Swadi, N. Bhattacharya, F. Mistree, and J. K. Allen</i>	315
Sensor Design for Automobile Air Gas Systems: Design Methods and Criteria <i>Ching-Yao Chan</i>	327
Robust Fatigue Design for Combined Bending and Steady Torsion <i>Rudolph J. Eggert</i>	335
Parametric Design of Low Lateral Force Rollers for Belt Loop Drives <i>David A. Hoeltzel, H. Richard Quadracci, and Vittorio Castelli</i>	343
MODELING OF VIBRATIONS AND IMPACT IN DYNAMIC SYSTEMS	
Chaotic Behavior of a Two Mass Bouncing System <i>Chi-Wook Lee, Ali Seireg, and Joseph Duffy</i>	361
Minimization of the Vibration Energy of Thin-Plate Structures <i>Katsumi Inoue, Dennis P. Townsend, and John J. Coy</i>	369
Occupant Dynamic Responses for Evaluation of Compliance Characteristics of Aircraft Bulkheads <i>Hamid M. Lankarani, Deren Ma, and Rajiv Menon</i>	377
Modeling and Dynamic Analysis of the Suspension System of a Front Loaded Washing Machine <i>O. S. Türkay, I. T. Sümer, and A. K. Tuğcu</i>	383
Hertz Contact Force Model With Permanent Indentation in Impact Analysis of Solids <i>Hamid M. Lankarani and Parviz E. Nikraves</i>	391
Tilt-Wing Rotorcraft Dynamic Analysis Using Multibody Formulation <i>Patrick J. O'Heron, Parviz E. Nikraves, Ara Arabyan, and Donald L. Kunz</i>	397
Author Index	403

SECOND ORDER DESIGN SENSITIVITY ANALYSIS OF KINEMATICALLY-DRIVEN MECHANICAL SYSTEMS

Qiushu Cao and Prakash Krishnaswami
Department of Mechanical Engineering
Kansas State University
Manhattan, Kansas

ABSTRACT

Second order design sensitivity information is required for several design applications, including second order optimization, minimum sensitivity design and reliability design. The problem of computing this information in a generalized manner becomes difficult when the dependence of system response on design is not explicitly known, as in the case of kinematic systems. This paper presents a general method for second order design sensitivity analysis of constrained mechanical systems. This method uses the constrained multi-element technique for kinematic analysis combined with a direct differentiation approach for obtaining first and second order design sensitivities of the system response. The method was implemented in a computer program on which several examples were solved. Three of the examples are presented in this paper. For each example, the second order sensitivities are checked against values obtained by finite differencing. In all cases, the agreement is seen to be very close, indicating that the proposed method is accurate and reliable.

INTRODUCTION

The response of a physical system is often described in terms of a set of appropriate state variables. Similarly, the parametric design of a system is usually described by a set of design variables. The response of the system is implicitly or explicitly dependent on the design variables. The evaluation of the partial derivatives of the state variables with respect to the design variables is called design sensitivity analysis. Most of the previous work that has been done is in the area of first order design sensitivity analysis, i.e., only the first order partial derivatives are computed. However, some applications require information about the corresponding second derivatives. In order to compute these, it is necessary to perform second order design sensitivity analysis of the system.

The second order design sensitivity information of a system can be utilized in a variety of ways. It has been shown that it can be used effectively for second order optimization of structural systems [1]. Second order sensitivity has also been used in the minimum sensitivity design of four bar linkages [2]. In addition, second order sensitivity has potential applications in optimal tolerancing and reliability design. Most previous work in second order sensitivity analysis has been very problem specific. In the area of mechanical systems, there has been some success in developing second order sensitivity analysis methods for specific [3] as well as generalized dynamic systems [4,5].

The work described in this paper is aimed at developing a generalized formulation for second order design sensitivity analysis of constrained kinematic systems. Such a system may be viewed as a collection of rigid bodies interconnected by joints. The technique that is employed for kinematic analysis is the constrained multi-element formulation [6]. In this formulation each rigid body is assigned six generalized coordinates (or three generalized coordinates if the system is planar). The generalized coordinates of all the bodies in the system are placed in a system generalized coordinate vector, denoted by \mathbf{q} . The system generalized velocity vector, $\dot{\mathbf{q}}$, and the system generalized acceleration vector, $\ddot{\mathbf{q}}$, are defined correspondingly.

The joints in the system are modeled by writing the kinematic constraint equations corresponding to each joint. These equations are nonlinear algebraic equations that are written in terms of the generalized coordinates. Standard kinematic constraint equations are available for describing revolute and translational joints [4,6]. Other types of joints can also be described by writing suitable constraint equations. In addition to the constraints imposed by the joints, a kinematically driven system must also have a set of kinematic driving functions; in fact, the number of driving equations must be exactly equal to the number of degrees-of-freedom of the system if the problem is well-posed. In the current formulation, these driving functions are also modeled by writing suitable kinematic constraints in

terms of the generalized coordinates. Most of the commonly encountered driving functions, such as constant velocity and constant acceleration drives, can be modeled in this way.

In order to perform second order design sensitivity analysis, a set of design variables must also be specified. This set can contain any parameters that do not vary with time. The most common choices for design variables are link lengths and/or locations of target points on links. Once the design variables are selected, they are placed in a design vector, denoted \mathbf{b} .

With these definitions, it may be seen that the problem of finding the second order design sensitivity of the response of a kinematic system can be viewed as the problem of computing the second order partial derivatives of the vectors \mathbf{q} , $\dot{\mathbf{q}}$ and $\ddot{\mathbf{q}}$ with respect to the design vector, \mathbf{b} . Using the subscript notation for partial derivatives, we can say that our task is to find the quantities \mathbf{q}_{bb} , $\dot{\mathbf{q}}_{bb}$, and $\ddot{\mathbf{q}}_{bb}$. Each of these terms is a transient quantity that must be evaluated at each instant (or configuration) at which the kinematic analysis is performed.

In some instances, it may be necessary to compute the design sensitivity of a set of performance functions of the system, instead of the system response itself. This situation can be easily handled once the second order design sensitivity of the system response is known, provided the performance functions are of the form $f(\mathbf{q}, \dot{\mathbf{q}}, \ddot{\mathbf{q}}, \mathbf{b}, \mathbf{t})$. The details of how this computation can be done may be found in [4].

KINEMATIC ANALYSIS

The governing equations of a kinematically driven system are constraint equations obtained from the joints and the driving functions. These equations can be written in the form:

$$\mathbf{G}(\mathbf{q}, \mathbf{b}, \mathbf{t}) = 0 \quad (1)$$

Where \mathbf{q} is the generalized coordinate,
 \mathbf{b} is the design variable vector and
 \mathbf{t} is the time.

Equation 1 represents a system of simultaneous nonlinear equations that can be solved by the Newton-Raphson iteration. The Newton updates for this are given by:

$$\mathbf{G}_q \Delta \mathbf{q} = -\mathbf{G} \quad (2)$$

To solve for velocities, Equation 1 is differentiated with respect to time to obtain the following relationship:

$$\mathbf{G}_q \dot{\mathbf{q}} = -\dot{\mathbf{G}}_t \quad (3)$$

Further differentiation of Equation 3 with respect to time yields a set of equations that can be solved to get accelerations:

$$\mathbf{G}_q \ddot{\mathbf{q}} = -\ddot{\mathbf{G}}_t - 2 \mathbf{G}_{q\dot{q}} - (\mathbf{G}_{q\ddot{q}}) \dot{\mathbf{q}} \quad (4)$$

Equation 2, 3, and 4 can thus be used to solve for the position, velocity and acceleration of the system. It should be noted that the coefficient matrix is the same in Equations 2,3, and 4. Thus, the matrix needs to be factored only once after the Newton-Raphson iteration converges; all subsequent solutions are done by direct forward and backward substitution. The entire solution process is repeated at every instant (or configuration) at which the response is desired.

DESIGN SENSITIVITY ANALYSIS

The technique that is adopted for performing design sensitivity analysis is the direct differentiation method [7] which has been used successfully for computing design sensitivities of constrained dynamic systems. The basic idea of this method is to differentiate the governing equations of the system to obtain a set of equations in terms of the corresponding sensitivity coefficients. The governing equations for a kinematic mechanical system are the kinematic constraints of Equation 1. Thus, following the direct differentiation approach, we differentiate both sides of Equation 1 with respect to each design variable and rearrange terms to obtain the following set equations:

$$\mathbf{G}_q \mathbf{q}_{b_j} = -\mathbf{G}_{b_j} \quad j=1, \dots, m \quad (5)$$

where m is the number of design variables.

Equation 5 can be directly solved to obtain the first order sensitivity coefficients of position. Furthermore, Equation 5 can be differentiated with respect to time to obtain a set of equations for the first order sensitivity coefficients of velocity:

$$\mathbf{G}_q \dot{\mathbf{q}}_{b_j} = -(\dot{\mathbf{G}}_q \mathbf{q}_{b_j} + \dot{\mathbf{G}}_{b_j}) \quad j=1, \dots, m \quad (6)$$

A further differentiation of Equation 6 with respect to time yields a solvable set of equations in the sensitivity coefficients of acceleration:

$$\mathbf{G}_q \ddot{\mathbf{q}}_{b_j} = -(2\dot{\mathbf{G}}_q \dot{\mathbf{q}}_{b_j} + \ddot{\mathbf{G}}_q \mathbf{q}_{b_j} + \ddot{\mathbf{G}}_{b_j}) \quad j=1, \dots, m \quad (7)$$

The direct differentiation strategy can be extended to obtain second order sensitivity information also. In this case, we must differentiate the first order sensitivity equations with respect to design to get a set of equations in the second order sensitivities. In order to do this, we first differentiate Equation 5 with respect to design and obtain a set of second order position sensitivity equations:

$$\mathbf{G}_q \mathbf{q}_{b_j b_k} = -(\mathbf{G}_q \ddot{\mathbf{q}}_{b_j})_q \mathbf{q}_{b_k} - (\mathbf{G}_q \ddot{\mathbf{q}}_{b_j})_{b_k} - \mathbf{G}_{b_j q} \mathbf{q}_{b_k} - \mathbf{G}_{b_j b_k} \quad (8)$$

$$j=1, \dots, m; \quad k=1, \dots, m$$

Similarly, Equation 6 can be differentiated with respect to design to get a set of second order velocity sensitivity equations:

$$\mathbf{G}_q \dot{\mathbf{q}}_{b_j b_k} = -(\mathbf{G}_q \ddot{\mathbf{q}}_{b_j})_q \mathbf{q}_{b_k} - (\mathbf{G}_q \ddot{\mathbf{q}}_{b_j})_{b_k} - (\dot{\mathbf{G}}_q \ddot{\mathbf{q}}_{b_j})_q \mathbf{q}_{b_k} - (\dot{\mathbf{G}}_q \ddot{\mathbf{q}}_{b_j})_{b_k} - \dot{\mathbf{G}}_q \mathbf{q}_{b_j b_k} - (\dot{\mathbf{G}}_q \dot{\mathbf{q}}_{b_j})_q \mathbf{u}_{b_k} + \dot{\mathbf{G}}_{b_j q} \mathbf{u}_{b_k} + \dot{\mathbf{G}}_{b_j b_k} \quad (9)$$

$$j=1, \dots, m; \quad k=1, \dots, m$$

Finally, Equation 7 can be differentiated with respect to design, resulting in a set of equations for the acceleration sensitivities:

$$\mathbf{G}_q \ddot{\mathbf{q}}_{b_j b_k} = -(\mathbf{G}_q \ddot{\mathbf{q}}_{b_j})_q \mathbf{q}_{b_k} - (\mathbf{G}_q \ddot{\mathbf{q}}_{b_j})_{b_k} - 2(\dot{\mathbf{G}}_q \ddot{\mathbf{q}}_{b_j})_q \mathbf{q}_{b_k} - 2(\dot{\mathbf{G}}_q \ddot{\mathbf{q}}_{b_j})_{b_k} \dot{\mathbf{q}}_{b_k} - 2(\dot{\mathbf{G}}_q \dot{\mathbf{q}}_{b_j})_{b_k} - 2\dot{\mathbf{G}}_q \dot{\mathbf{q}}_{b_j b_k} - (\ddot{\mathbf{G}}_q \ddot{\mathbf{q}}_{b_j})_q \mathbf{q}_{b_k} - (\ddot{\mathbf{G}}_q \ddot{\mathbf{q}}_{b_j})_{b_k} \dot{\mathbf{q}}_{b_k} - (\ddot{\mathbf{G}}_q \dot{\mathbf{q}}_{b_j})_q \ddot{\mathbf{q}}_{b_k} - (\ddot{\mathbf{G}}_q \dot{\mathbf{q}}_{b_j})_{b_k} - \ddot{\mathbf{G}}_{b_j q} \mathbf{q}_{b_k} - \ddot{\mathbf{G}}_{b_j b_k} \dot{\mathbf{q}}_{b_k} - \ddot{\mathbf{G}}_{b_j q} \dot{\mathbf{q}}_{b_k} - \ddot{\mathbf{G}}_{b_j b_k} \quad (10)$$

$$j=1, \dots, m; \quad k=1, \dots, m$$

It is worth noting that Equations 5 through 10 all have the same

coefficient matrix, G_g . As noted earlier, this matrix is already available in factored form. Thus, the calculation of the first and second order sensitivity coefficients can be performed very efficiently if they are done concurrently with the kinematic analysis.

NUMERICAL EXAMPLES

The methods presented in the preceding section were implemented in a computer program. Three example problems that were solved using this program are presented in this section. All problem dependent FORTRAN subroutines were generated automatically using the symbolic computing language REDUCE-3. For all the three problems, the system response as well as the first and second order design sensitivity coefficients were computed. The first and second order sensitivities were checked by comparing them against values obtained using a finite difference method. The results of this check are plotted for one selected coordinate for each example. It was found that the difference between the two methods was never greater than 1%.

Example 1: Double Slider Mechanism

The initial assembly and design variables of a double slider mechanism are shown in Figure 1. Only self weight is acting on the system. The simulation time is from 0 to 1 second. The initial data (in MKS) are:

Masses:

$$m_1 = 8.0; \quad m_2 = 8.0;$$

Moments of inertia:

$$J_1 = 8.0; \quad J_2 = 8.0;$$

Design vector:

$$b = [1.4142];$$

The initial position:

$$y_1 = 1.0\text{m};$$

The initial velocity:

$$\dot{y}_1 = 0.2 \text{ m/s}.$$

The driving function:

$$\dot{y}_1 = 0.2 = 0.0$$

The second order sensitivity results for the position and acceleration of the horizontal slider are plotted in Figure 2 and 3 respectively. The sensitivities obtained by finite difference are also shown in each figure. It is seen that the analytical second order sensitivity curve and the finite difference second order sensitivity curve lie almost exactly on top of each other, thus appearing as a single curve in the plots.

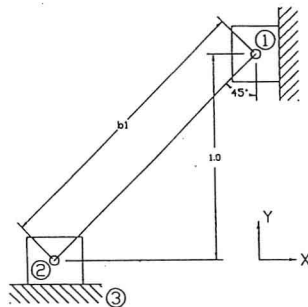


Figure 1: Double slider Mechanism (Example 1)

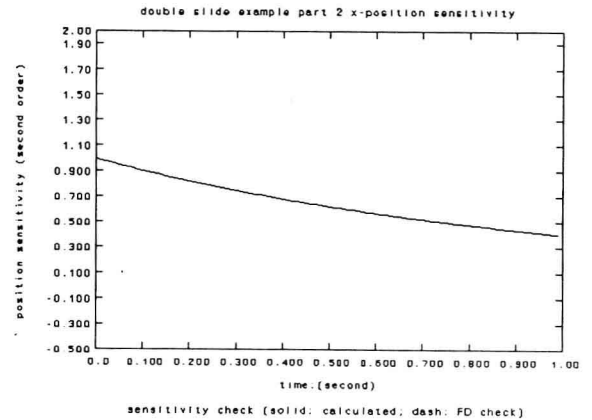


Figure 2: Finite difference check on second order sensitivity of position of link 2, example 1

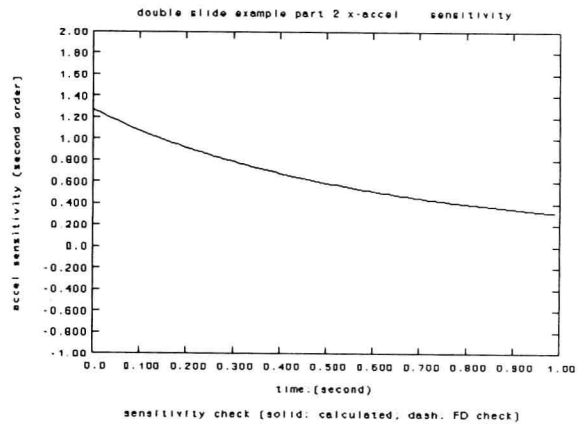


Figure 3: Finite difference check on second order sensitivity of acceleration of link 2, example 1

Example 2: Slider-Crank Mechanism

The initial assembly and design variables of the problem are shown in Figure 4. A force $F = 125\text{N}$ is applied to the piston as shown. The only other forces are the weights of the members. The simulation time is from 0 to 1 second.

Masses:

$$m_1 = 5.0; \quad m_2 = 15.0; \quad m_3 = 3.0;$$

Moment of Inertia:

$$J_1 = 0.5; \quad J_2 = 2.5; \quad J_3 = 8.0;$$

Design variables:

$$b = [0.25, 0.25]^T$$

Initial velocity:

$$\phi_1 = 1 \text{ rad/s}.$$

Driving function:

$$\phi_1 = (\pi/4) + 0.05 * t ** 2$$

The second order sensitivity results for the position and acceleration of the slider are plotted in Figures 5 and 6 respectively. The sensitivities obtained by finite difference lie almost exactly on top of the analytical second order sensitivities.

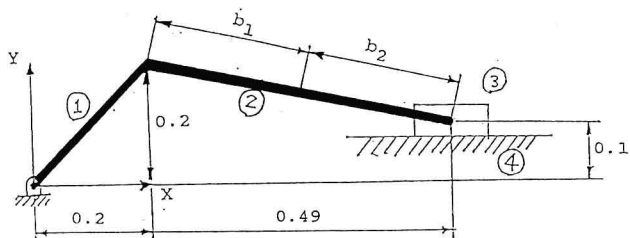


Figure 4: Slider-Crank Mechanism (Example 2)

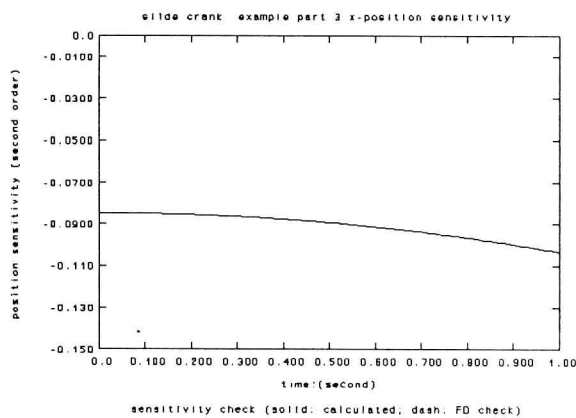


Figure 5: Finite difference check on second order sensitivity of position of link 3, Example 2.

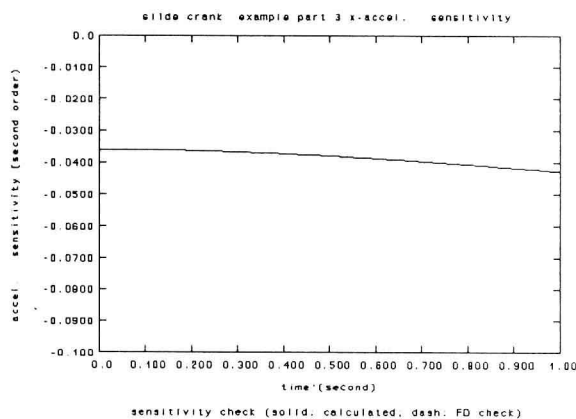


Figure 6: Finite difference check on second order sensitivity of acceleration of link 3, Example 2.

Example 3: Quick Return Mechanism

The initial assembly and design variables are shown in figure 7.

Masses:

$$m_1 = 8.0; m_2 = 1000.0; m_3 = 100.0; m_4 = 30.0; m_5 = 50;$$

Moment of Inertia:

$$J_1 = 8.0; J_2 = 2000.0; J_3 = 100.0; J_4 = 10.0; J_5 = 1.5$$

Design variables:

$$b = [1.5 \ 2.0 \ 2.0 \ 1.9]^T$$

Initial position:

$$\phi_3 = 0.0 \text{ rad.}$$

Initial acceleration:

$$\phi_1 = 0.1 \text{ rad/s}^2.$$

Driving function:

$$\phi_3 = 0.05 * t$$

The results are shown in Figure 8 and 9 respectively. Like the previous two examples, there is very good agreement between the analytical second order sensitivities and the sensitivities obtained by finite difference.

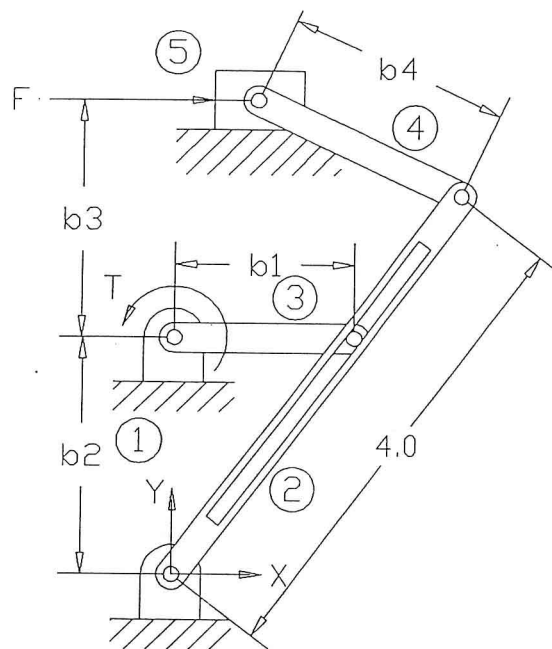


Figure 7: Quick Return Mechanism (example 3)

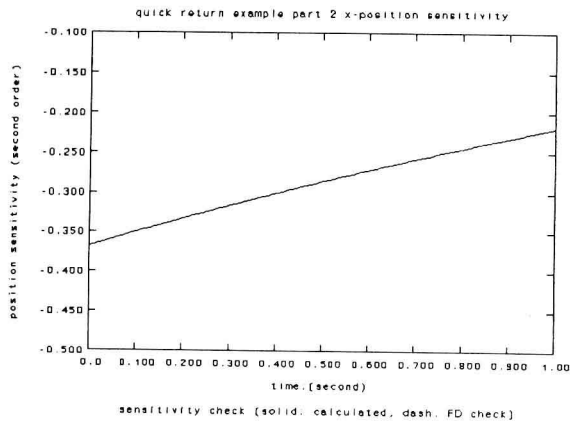


Figure 8: Finite difference check on second order sensitivity of position of link 2, example 3.

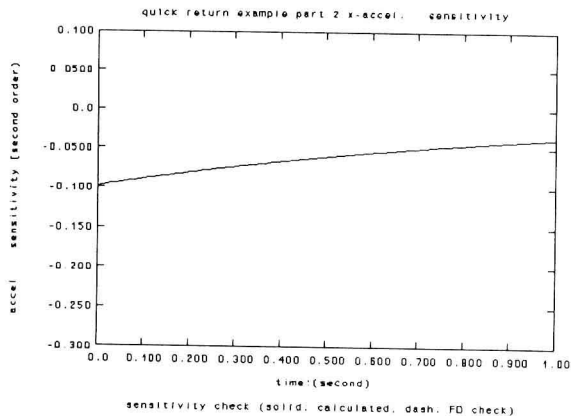


Figure 9: Finite difference check on second order sensitivity of acceleration of link 2, example 3.

REFERENCES

1. Haftka, R.T. and Starners, J.H., "Applications of a Quadratic Extended Interior Penalty Function for Structural Optimization", AIAA Journal, Vol. 14, No. 6, June, 1976.
2. Erickson, D., "Minimum Sensitivity Design of Four Bar Linkages", Masters Thesis, Dept. of Mech. Engg., Kansas State University, 1988.
3. Haug, E.J. and Ehle, P., "Second order Design Sensitivity Analysis for Mechanical System Dynamics", International Journal for Numerical Methods in Engineering, Vol. 18, 1982.
4. Haug, E.J., Mani, N.K. and Krishnaswami, P., "Design Sensitivity Analysis and Optimization of Dynamically Driven Systems", Computer-Aided Analysis and Optimization of Mechanical System Dynamics, Springer-Verlag, 1984.
5. Ramaswamy, S., "Supercomputer Based Second Order Design Sensitivity analysis of Constrained Dynamic Systems", Masters Thesis, Dept. of Mech. Engg., Kansas State University, 1988.
6. Orlandea, N., Chance, M.A. and Callahan, C.A., "A Sparsity Oriented Approach to the Dynamic Analysis and Design of Mechanical Systems, Parts I and II", ASME Journal of Engineering for Industry, Ser. B., Vol. 99, 1977.
7. Tomovic, R., Sensitivity Analysis of Dynamic Systems, McGraw-Hill, New York, 1963.

DETERMINATION OF SIGNIFICANCE OF STRESS STIFFENING EFFECTS IN FLEXIBLE MULTIBODY DYNAMIC SYSTEMS

Jeha Ryu, Sang Sup Kim, and Sung-Soo Kim
Department of Mechanical Engineering
Center for Simulation and Design Optimization
of Mechanical Systems
University of Iowa
Iowa City, Iowa

ABSTRACT

This paper presents a criterion for determining whether or not a flexible multibody dynamic system reveals stress stiffening effects. In the proposed criterion, the eigenvalue variation that results from adding the modal stress stiffness matrix to the conventional linear modal stiffness matrix is examined numerically before actual dynamic simulation. If the variation is sufficiently large for any flexible body, then stress stiffening effects are said to be significant and must be included in dynamic simulation of flexible multibody systems. Since the criterion uses the most general stress stiffness matrix, which can be represented as a function of applied and constraint reaction loads as well as of a system of 12 inertial loads, this criterion is applicable to any general flexible multibody dynamic systems. Several numerical results are presented to show the effectiveness of the proposed criterion.

1. INTRODUCTION

Modern mechanical systems such as spacecraft, satellites, mechanisms, and robotic manipulators are typically light, fast, precise, and complex in order to reduce material and power costs and to increase performance. Dynamic analysis of such systems requires not only proper account of both gross body motion and concurrent small elastic deformation of flexible bodies but also accurate inclusion of the important coupling effects existing between these two modes of dynamic behavior (Kane et al. 1987). One of the important coupling effects, so called *stress stiffening effects*, arises from the variations in flexible body stiffness induced by inertial, internal constraint, and external loads. For example, the tip deflection of a spinning beam modeled without including stiffness variations resulting from a centrifugal force will diverge as the spin rate approaches the quiescent natural frequency of the first bending mode.

During the last decade, several approaches have been proposed to incorporate stress stiffening effects into dynamic formulations of flexible multibody systems. These approaches are summarized by Ryu (1991), who suggested a method of computing the most general stress stiffness matrix of an arbitrary flexible body undergoing large gross motion accompanied by small elastic deformation. This stress stiffness matrix, represented as a function of applied and constraint reaction loads as well as of a

system of 12 inertial loads distributed throughout the flexible body, can be preprocessed by a readily available finite element analysis program for general structures.

Practical importance of stress stiffening effects, however, has been debated because these effects are not always significant in every mechanical system, and moreover, general inclusion of stress stiffening terms in the system equations of motion may not be a simple and inexpensive task (London, 1989; and Kane et al., 1989). Despite this disagreement, it is agreed that a good criterion would be very useful for determining the significance of stress stiffening effects. In other words, it will be very useful to know before actual dynamic simulation whether or not a given flexible multibody system reveals stress stiffening effects.

Very recently, Padilla and Flotow (1991) proposed a criterion for judging significance of stress stiffening effects for open-chain flexible multibody systems when they were investigating simple bounds on the applicability of their linearized equations of motion. According to their criterion, stress stiffening effects are not important if any prescribed motion of the body fixed reference frame is much smaller than the ratio of the minimum singular value of the conventional linear modal stiffness matrix to the maximum singular value of the modal stress stiffness matrix associated with this prescribed motion. It seems, however, that this criterion may not be applicable to systems with more than one motion and load because the resultant stress stiffening effects are generally a function of externally applied loads, body motion, and constraint reaction loads, which are usually unknown values prior to actual simulation. In addition, because flexible multibody dynamic systems are usually highly nonlinear, this simple bound on the magnitude of one of the motions of the body fixed reference frame does not sufficiently answer the question of how small the ratio must be in order not to show the stress stiffening effects in the final elastic displacements or stresses.

Another type of criterion for determining significance of stress stiffening effects can be devised by simply comparing an input speed with the first natural frequency of a whole system. This kind of rule-of-thumb criterion has been used widely in determining whether or not rigid body dynamic simulation combined with quasi-static structural analysis is valid in order to avoid solving more complex coupled equations of motion (Lowen and Chassapis, 1986). Following the logic used in this criterion, for example, stress stiffening effects are not anticipated if a constant input crank speed of a closed loop flexible four-bar mechanism is far smaller than the first bending natural frequency

of the whole system. However, it seems that this criterion may not be useful for a system with time-varying input speeds and with the configuration-dependent first natural frequency of mechanisms. To the authors' knowledge, a generally applicable criterion for complex flexible multibody dynamic systems has not been developed until now.

The objective of this paper is to present a generally applicable and practical criterion for determining when stress stiffening effects become significant in dynamic simulation of constrained flexible multibody systems. In section 2, the variational principle is used to derive Cartesian equations of motion of a flexible body that include stress stiffening terms. A finite element based method that is applicable to general and complex structures is also summarized to compute the stress stiffening terms. Section 3 presents a criterion based on the stress stiffness matrix to check the significance of stress stiffening effects. In section 4, several numerical examples are presented to demonstrate the validity and effectiveness of the proposed criterion. Finally, some conclusions and recommendations are made in section 5.

2. EQS. OF MOTION WITH STRESS STIFFENING TERMS

2.1 Variational Equations of Motion of a Flexible Body

Since a stress stiffness matrix plays a key role in setting up the criterion for judging the significance of stress stiffening effects in a later section, variational equations of motion of a flexible body are derived with the objectives of defining a stress stiffness matrix and of explaining how this stress stiffness matrix is incorporated into the dynamic equations of motion of a flexible body. The variational principle and the linear theory of elasticity are used in this derivation. In addition, in order to systematically include stress stiffening effects, nonlinear quadratic terms in the strain-displacement relationship are included in the internal virtual work.

Consider a flexible body that is in dynamic equilibrium in the deformed configuration as shown in Fig. 1. In this figure, the \underline{X} - \underline{Y} - \underline{Z} coordinate system is the inertial reference frame and the x - y - z coordinate system is the body reference frame in an undeformed configuration. Throughout the following derivations, bold letters denote vectors or matrices. An underlined variable is measured in the inertial reference frame, while other variables are measured in a local body reference frame.

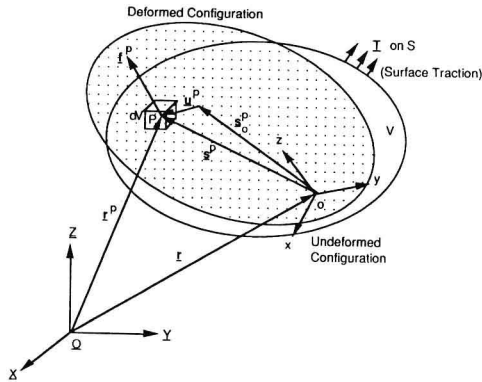


Figure 1 Undeformed and Deformed Configurations of a Flexible Body

The variational equations of motion of a flexible body are given as (Washizu, 1982)

$$\int_V \delta \underline{r}_i^p (\underline{f}_i^p - \rho \underline{\ddot{r}}_i^p) dV + \int_S \delta \underline{r}_i^p \underline{T}_i^p dS = \int_V \delta \underline{\epsilon}_{ij}^p \underline{\tau}_{ij}^p dV \quad (1)$$

where $\delta \underline{r}_i^p$ is the virtual displacement of point p that is consistent with constraints; \underline{f}_i^p is the body force density at point p ; ρ is the mass density; $\underline{\ddot{r}}_i^p$ is the acceleration of point p ; \underline{T}_i^p is an applied surface traction at point p ; $\underline{\tau}_{ij}^p$ is the second Piola-Kirchhoff stress tensor; $\delta \underline{\epsilon}_{ij}^p$ is the variation of the Green-Lagrange strain tensor consistent with given boundary conditions; and V and S are the volume and surface of the body before it is deformed. Dots over a vector in Eq. (1) and in the following derivations denote the total differentiation with respect to time.

Stress stiffening terms are derived from the virtual work done by internal forces. This virtual work is rewritten here as

$$\delta U = \int_V \delta \underline{\epsilon}_{ij}^p \underline{\tau}_{ij}^p dV \quad (2)$$

The virtual Green-Lagrange strain tensor can be written as

$$\delta \underline{\epsilon}_{ij} = \delta \underline{\epsilon}_{ij}^L + \delta \underline{\epsilon}_{ij}^N \quad (3)$$

where

$$\delta \underline{\epsilon}_{ij}^L = (1/2)(\delta u_{i,j} + \delta u_{j,i}) \quad (4)$$

$$\delta \underline{\epsilon}_{ij}^N = \delta u_{k,i} u_{k,j} \quad (5)$$

Note that superscript p of $\delta \underline{\epsilon}_{ij}^p$ and $\underline{\tau}_{ij}^p$, and of the deformational displacement vector \underline{u}^p is omitted for notational convenience in Eqs. (3) through (5) and in the following derivations.

The second Piola-Kirchhoff stresses are assumed to be composed of incremental stresses resulting from dynamic deformation and reference stresses, which are assumed to be induced by D'Alembert inertial loads arising from the gross body motion of the body reference frame, externally applied loads, and constraint reaction loads in the undeformed configuration of a flexible body. The reference stresses are considered as those stresses that existed in a flexible body in the undeformed configuration, that is, before the start of a deformation of interest (Washizu, 1982). If the linear strain-stress relationship is assumed for a homogeneous and isotropic material, the second Piola-Kirchhoff stress tensor can be written as

$$\underline{\tau}_{ij} = D_{ijkl} \underline{\epsilon}_{kl} + \underline{\tau}_{ij}^r \quad (6)$$

where D_{ijkl} is the constitutive tensor, $\underline{\epsilon}_{kl}$ is the linear strain tensor, and $\underline{\tau}_{ij}^r$ is the reference stress tensor.

Substitution of the virtual strain tensor in Eq. (3) and the stress tensor in Eq. (6) into the internal virtual work of Eq. (2) yields

$$\delta U = \int_V \delta \underline{\epsilon}_{ij}^L D_{ijkl} \underline{\epsilon}_{kl}^L dV + \int_V \delta \underline{\epsilon}_{ij}^L \underline{\tau}_{ij}^r dV + \int_V \delta u_{k,i} \underline{\tau}_{ij}^r u_{k,j} dV \quad (7)$$

where the quadratic term is neglected.

Assume that the elastic displacement vector \underline{u} at point p is expressed as a linear combination of the time-dependent deformation modal coordinate vector \underline{a} and the space-dependent mode shape matrix $\Phi^p(\underline{s}_0^p)$ defined at point p of the undeformed body; i.e.,

$$\underline{u}(\underline{s}_0^p, t) = \Phi^p(\underline{s}_0^p) \underline{a}(t) \quad (8)$$

Then, by substituting Eq. (8) into Eqs. (4), (5) and (7), Eq. (7) can be rewritten as

$$\delta U = \delta \underline{a}^T (\underline{K}^L + \underline{K}^N) \underline{a} + \delta \underline{a}^T \underline{F}^r \quad (9)$$

where \mathbf{K}^z is the conventional linear modal stiffness matrix, \mathbf{K}^n is the modal stress stiffness matrix, and \mathbf{F}^r is an additional force vector (Bathe, 1982). The terms in Eq. (9) are defined as

$$\mathbf{K}^z = \int_V \mathbf{B}^{zT} \mathbf{D} \mathbf{B}^z dV, \text{ with } \mathbf{B}^z = \mathbf{L} \Phi^P \quad (10)$$

$$\mathbf{K}^n = \int_V \mathbf{B}^{nT} \mathbf{T} \mathbf{B}^n dV, \text{ with } \mathbf{B}^n = \nabla \Phi^P \quad (11)$$

$$\mathbf{F}^r = \int_V \mathbf{B}^{zT} \boldsymbol{\tau}^r dV \quad (12)$$

where differential operator matrices \mathbf{L} and ∇ , and a (9×9) stress matrix \mathbf{T} are defined in Ryu (1991).

The variational equations of motion of a flexible body that include stress stiffening terms are given in matrix form as (Ryu, 1991)

$$[\delta \mathbf{r}^T, \delta \boldsymbol{\pi}^T, \delta \mathbf{a}^T] \left\{ \mathbf{M} \begin{bmatrix} \ddot{\mathbf{r}} \\ \dot{\boldsymbol{\omega}} \\ \ddot{\mathbf{a}} \end{bmatrix} + \mathbf{S} + \mathbf{V} - \mathbf{Q} \right\} = 0 \quad (13)$$

for $\delta \mathbf{r}$, $\delta \boldsymbol{\pi}$, and $\delta \mathbf{a}$ that are consistent with constraints acting on the flexible body, where $\delta \mathbf{r}$ is the virtual displacement of the origin of the body reference frame; $\delta \boldsymbol{\pi}$ is the virtual rotation of the body reference frame; $\delta \mathbf{a}$ is the variation of a deformation

modal coordinate vector; $\ddot{\mathbf{r}}$, $\dot{\boldsymbol{\omega}}$, and $\ddot{\mathbf{a}}$ are translational acceleration, angular velocity, and angular acceleration vectors of the body reference frame. The entries in matrix \mathbf{M} and vectors \mathbf{S} and \mathbf{Q} are presented in Ryu (1991).

The generalized internal force vector \mathbf{V} , derived from the virtual work, is defined as

$$\mathbf{V}(\mathbf{a}, \boldsymbol{\tau}^r) = \begin{bmatrix} 0 \\ 0 \\ (\mathbf{K}^z + \mathbf{K}^n) \mathbf{a} + \mathbf{F}^r \end{bmatrix} \quad (14)$$

Note that the time-varying stress stiffness matrix \mathbf{K}^n and an additional force vector \mathbf{F}^r are added to the generalized internal force vector \mathbf{V} in comparison with the conventional flexible body equations of motion (Wu et al., 1989).

2.2 Computation of Stress Stiffening Terms

As shown in Eq. (11), the stress stiffness matrix \mathbf{K}^n is a function of the reference stress state that exists before deformation of a flexible body. This stress state is assumed to be induced from D'Alembert inertial loads resulting from gross body motion described by the motion of the body reference frame as well as from externally applied loads and constraint reaction loads resulting from the motion of adjacent bodies. Since the linear theory of elasticity is assumed in defining the reference stress state, the stress stiffness matrix via the reference stress state can be obtained by a standard linear structural analysis (Cook, 1985).

Here, the procedure proposed by Ryu et al. (1991) is used to obtain the stress stiffness matrix through a series of structural analyses. In this procedure, quasi-static structural analyses generate the stress stiffness influence coefficient matrices $\hat{\mathbf{K}}_i^n$

associated with unit values of 12 time-dependent terms ($\ddot{r}_x, \ddot{r}_y, \ddot{r}_z, \dot{\omega}_x, \dot{\omega}_y, \dot{\omega}_z, \omega_x^2, \omega_y^2, \omega_z^2, \omega_x \omega_y, \omega_y \omega_z, \omega_z \omega_x$). These terms are defined by representing the inertial loads induced by gross body

motion as a combination of space-dependent and time-dependent terms. Then, a stress stiffness matrix $\hat{\mathbf{K}}_A^n$ resulting from the gross body motion of the flexible body is obtained by applying the superposition principle:

$$\hat{\mathbf{K}}_A^n = \ddot{r}_x \hat{\mathbf{K}}_1^n + \ddot{r}_y \hat{\mathbf{K}}_2^n + \ddot{r}_z \hat{\mathbf{K}}_3^n + \dot{\omega}_x \hat{\mathbf{K}}_4^n + \dot{\omega}_y \hat{\mathbf{K}}_5^n + \dot{\omega}_z \hat{\mathbf{K}}_6^n + \omega_x^2 \hat{\mathbf{K}}_7^n + \omega_y^2 \hat{\mathbf{K}}_8^n + \omega_z^2 \hat{\mathbf{K}}_9^n + \omega_x \omega_y \hat{\mathbf{K}}_{10}^n + \omega_y \omega_z \hat{\mathbf{K}}_{11}^n + \omega_z \omega_x \hat{\mathbf{K}}_{12}^n \quad (15)$$

In case of the externally applied and constraint reaction loads, static structural analyses generate the stress stiffness influence coefficient matrix associated with each time-invariant unit load in each coordinate axis of the body reference frame. Then, a stress stiffness matrix $\hat{\mathbf{K}}_B^n$ resulting from applied and constraint reaction loads is obtained as

$$\hat{\mathbf{K}}_B^n = \sum_i^{\text{naf}} (\mathbf{T}_{xi}^a \hat{\mathbf{K}}_{axi}^n + \mathbf{T}_{yi}^a \hat{\mathbf{K}}_{ayi}^n + \mathbf{T}_{zi}^a \hat{\mathbf{K}}_{azi}^n) + \sum_j^{\text{ncl}} (\mathbf{T}_{xj}^c \hat{\mathbf{K}}_{cxj}^n + \mathbf{T}_{yj}^c \hat{\mathbf{K}}_{cyj}^n + \mathbf{T}_{zj}^c \hat{\mathbf{K}}_{czj}^n) + f_x^b \hat{\mathbf{K}}_1^n + f_y^b \hat{\mathbf{K}}_2^n + f_z^b \hat{\mathbf{K}}_3^n \quad (16)$$

for the body force f^b , applied concentrated loads \mathbf{T}^a , and constraint reaction loads \mathbf{T}^c , where naf and ncl are number of applied and constraint reaction loads, respectively. The subscripts x, y, and z denote each body coordinate axis.

By combining the stress stiffness matrices $\hat{\mathbf{K}}_A^n$ in Eq. (15) and $\hat{\mathbf{K}}_B^n$ in Eq. (16), the total modal stress stiffness matrix \mathbf{K}^n is obtained as

$$\mathbf{K}^n = \hat{\Phi}^T (\hat{\mathbf{K}}_A^n + \hat{\mathbf{K}}_B^n) \hat{\Phi} \quad (17)$$

where $\hat{\Phi}$ is the $(n \times m)$ modal matrix in the nodal space, and where n and m are the total number of nodal degrees-of-freedom and modal coordinates, respectively.

Up to here, only computation of stress stiffness matrix \mathbf{K}^n in Eq. (11) has been explained. The additional force term \mathbf{F}^r in Eq. (12) can be computed in exactly the same way as the computation of \mathbf{K}^n because the superposition principle can also be applied.

2.3 System Eqs. of Motion with Stress Stiffening Terms

System equations of motion of a flexible multibody system can be derived from the variational equations of motion of a flexible body in Eq. (13) using either a relative joint coordinate formulation or an absolute Cartesian coordinate formulation. For a constrained flexible multibody system, a general form of dynamic equations of motion can be represented as (Wu et al., 1989)

$$\hat{\mathbf{M}} \ddot{\mathbf{q}} + \boldsymbol{\Psi}_q^T \boldsymbol{\lambda} = \hat{\mathbf{Q}} \quad (18)$$

where $\hat{\mathbf{M}}$, \mathbf{q} , $\boldsymbol{\Psi}_q$, $\boldsymbol{\lambda}$, and $\hat{\mathbf{Q}}$ are the system generalized mass matrix, the system generalized coordinate vector, the system constraint Jacobian matrix, the unknown Lagrangian multiplier vector associated with constraints, and the system generalized force vector, respectively. Note that the system generalized force vector $\hat{\mathbf{Q}}$ contains the stress stiffening force.

In addition to Eq. (18), constraint acceleration equations are needed in order to uniquely solve the unknowns $\ddot{\mathbf{q}}$ and $\boldsymbol{\lambda}$. These equations can be expressed as (Haug, 1989)

$$\boldsymbol{\Psi}_q \ddot{\mathbf{q}} = -(\boldsymbol{\Psi}_q \dot{\mathbf{q}})_q \dot{\mathbf{q}} - 2\boldsymbol{\Psi}_{qt} \dot{\mathbf{q}} - \boldsymbol{\Psi}_{tt} = \boldsymbol{\gamma} \quad (19)$$

where subscripts t and q denote partial differentiation with respect to time and vector q, respectively. By combining Eqs.

(18) and (19), the system dynamic equations of motion can be written in matrix form as

$$\begin{bmatrix} \dot{\mathbf{M}} & \Psi^T \mathbf{q} \\ \Psi \mathbf{q} & 0 \end{bmatrix} \begin{bmatrix} \ddot{\mathbf{q}} \\ \dot{\lambda} \end{bmatrix} = \begin{bmatrix} \dot{\mathbf{Q}} \\ \mathbf{y} \end{bmatrix} \quad (20)$$

The solution and the integration of Eq. (20) give histories of the acceleration of system generalized coordinates and Lagrangian multipliers. From these data, constraint reaction loads are derived via the Lagrangian multipliers (Kim and Haug, 1989). Then these values can be used to update the stress stiffness matrix defined in Eqs. (15) and (16) at the current time step (Ryu et al., 1991).

3. CRITERION FOR DETERMINING THE SIGNIFICANCE OF STRESS STIFFENING EFFECTS

Stress stiffening effects must be included in dynamic simulation of a flexible multibody system whenever the addition of the stress stiffness to the conventional linear stiffness results in a significant variation of the stiffness of the system. However, general inclusion of stress stiffening terms in the system equations of motion may not be a simple and inexpensive task. Therefore, it will be very useful to know whether or not a given flexible multibody system reveals stress stiffening effects before actual dynamic simulation.

This section presents a criterion for determining the significance of stress stiffening effects in flexible multibody dynamic systems using the stress stiffness matrix derived in the previous section. Unlike the criterion proposed by Padilla and Flotow (1991), the proposed criterion is applicable to general flexible multibody systems with closed loops. Briefly speaking, stress stiffening effects become significant when a mechanical system operates at a high speed, and/or when a deformable body is very flexible even at a low speed, and/or when large magnitude loads act on a deformable body. This can be seen in the derivation of the stress stiffness matrix of a flexible body because, as Eqs. (15) and (16) show, the total stress stiffness matrix is a function of (a) geometry of the flexible body, which is used in defining the stress stiffness influence coefficient matrices, (b) linear and angular accelerations and angular velocities of the body reference frame, (c) applied loads, and (d) constraint reaction loads. Quantitative questions then arise about speed, flexibility, and magnitude of acting loads, which make significant contributions to the change of stiffness, and which in turn, results in significant changes in the final outputs such as elastic displacements or dynamic stresses. In order to answer these questions, other questions must be resolved first:

(i) how can stiffness variation be measured with addition of the stress stiffness?, and (ii) how much change in stiffness does significantly change final elastic displacements and stresses?

Since the stiffness of a flexible body changes by addition of stress stiffness, as seen in Eq. (14), the amount of variation of stiffness of a flexible body can be measured by the variation of the eigenvalues of the total modal stiffness matrix of the flexible body that results from the addition of the modal stress stiffness matrix. Note that the stiffness variation is examined body by body rather than for the total system, even in a multibody system, because stress stiffness variation in a body affects the stiffness variation of the system. In the measurement of stiffness variation, the modal stiffness instead of the nodal stiffness matrix is used because the generalized elastic force vector in Eq. (14) is represented in the modal space and because the size of the modal stiffness matrix is much smaller than that of the nodal stiffness matrix.

For a flexible body with time-varying modal stiffness matrix $\mathbf{K}(t)$, the characteristic equation of the eigenvalue problem is given as

$$\text{DET}(\mathbf{K}(t) - \lambda(t)\mathbf{I}) = 0 \quad (21)$$

where DET means the determinant operator, \mathbf{I} is an identity matrix, and $\lambda(t)$ is a time-varying eigenvalue associated with the time-varying total modal stiffness matrix $\mathbf{K}(t)$. This matrix consists of the time-invariant linear conventional modal stiffness \mathbf{K}^L and the time-varying modal stress stiffness matrix $\hat{\mathbf{K}}^n$. The total modal stiffness matrix can then be represented symbolically as

$$\mathbf{K}(t) = \mathbf{K}^L + \sum_i c_i(t) \hat{\mathbf{K}}_i^n \quad (22)$$

where $c_i(t)$ are the time-varying scalar coefficients shown in Eqs. (15) and (16).

The amount of variation of the stiffness of a flexible body can be measured by a time-varying ratio between the eigenvalues of the matrices $\mathbf{K}(t)$ and \mathbf{K}^L . This is defined as

$$R_1(t) = \frac{\lambda(t) \text{ from } \mathbf{K}(t)}{\lambda^L \text{ from } \mathbf{K}^L} \quad (23)$$

where $\lambda(t)$ and λ^L are one of the eigenvalues of the total modal stiffness matrix $\mathbf{K}(t)$ and the conventional linear modal stiffness matrix \mathbf{K}^L , respectively. Since the first eigenvalue of a matrix is usually the largest in many systems, $R_1(t)$ is usually defined for the first eigenvalue. Note that eigenvalue $\lambda(t)$ must be computed from Eq. (21) at every time step. The cost in computing this, however, is not expensive because the size of matrix $\mathbf{K}(t)$ is usually small for each flexible body.

In order to avoid computing the eigenvalues at every time step, another ratio $R_2(t)$ may be used as an alternative to ratio $R_1(t)$. The alternative ratio $R_2(t)$ is defined as

$$R_2(t) = 1.0 + \sum_i c_i(t) \frac{\lambda_i^n \text{ from } \hat{\mathbf{K}}_i^n}{\lambda^L \text{ from } \mathbf{K}^L} \quad (24)$$

Note that ratio $R_2(t)$ is an algebraic sum of the contribution of the eigenvalue variation resulting from each stress stiffness influence coefficient matrix. Since eigenvalues λ_i^n from the stress stiffness influence coefficient matrices $\hat{\mathbf{K}}_i^n$ are time-invariant, computation of $R_2(t)$ is much cheaper than that of $R_1(t)$. If the stiffness variation is not significant, then either ratio should be close to unity at any time. If at some time, either ratio is far from unity, then it can be said that stress stiffening effects may be significant. Note that a near-zero ratio implies that buckling may occur due to compressive forces.

For a single flexible body with prescribed gross body motion, the above ratios can be preprocessed before actual simulation because the coefficients $c_i(t)$ are known variables. For multibody systems, however, some of the coefficients $c_i(t)$, such as linear and angular accelerations of the body reference frame and constraint reaction loads, are usually unknown before actual dynamic simulation of the flexible multibody systems in which stress stiffening effects might be included. In this case, these unknown values may be approximately obtained by a rigid body dynamic simulation, which usually generates mean values on which flexibility effects are superimposed. Even though the values $c_i(t)$ from rigid and flexible body dynamic simulations are very different for a very flexible multibody system, the ratios based on rigid body approximations can still give good measures because overall trends may not be much different. Numerical results in section 4 demonstrate that either ratios can be used as a practical measure to check whether or not the system reveals stress stiffening effects.